

Supporting Information

Hierarchical dual-nanonet of polymer nanofibers and supramolecular nanofibrils for air filtration with high filtration efficiency, low air resistance and high moisture permeation

Maorui Hu, Yifei Wang, Zhifeng Yan, Guodong Zhao, Yixia Zhao, Lei Xia, Bowen Cheng, Youbo Di and Xupin Zhuang

Materials

Polyacrylonitrile (Mw=35000) was given by Sinopec Qilu Petrochemical Company. Dimethylformamide, n-propanol, ethylene glycol, and n-octyl alcohol were purchased from Tianjin Fengfan Chemical Reagent Technology Co, Ltd. All solvents were of analytical grade and used without further purification. 1,3:2,4-Di(3,4-dimethylbenzylidene) sorbitol (DMDBS) was synthesized according to the methods reported previously.¹

Solution blowing of PAN nanofiber mats

A pilot-plant equipment of 1.2 m (Fig. S1) in cross-direction was used for spinning of PAN nanofiber mats. A special homebuilt die (Fig. 1g) with 120 annular spinning orifices co-axially surrounded by individual gas cavity was used. The spinning procedures was reported previously. A 20 wt.% PAN solution in *N,N*-dimethylformamide (DMF) was fed to the orifices at a feed rate of 16 mL/h per orifice, and the compressed air was supplied to the gas cavities under 0.6 MPa. After the solution streams were pressed out of the orifices (0.38 mm in diameter), they were stretched to the extreme by high-velocity gas flow to jets. Then, nanofibers were obtained with solvent evaporation. The nanofiber mat was collected on a 12 g/m² polypropylene spunbond nonwoven fabric. The PAN nanofiber mat used in this study was 15.2 g/m². It was peeled off from the collector for the following procedures.

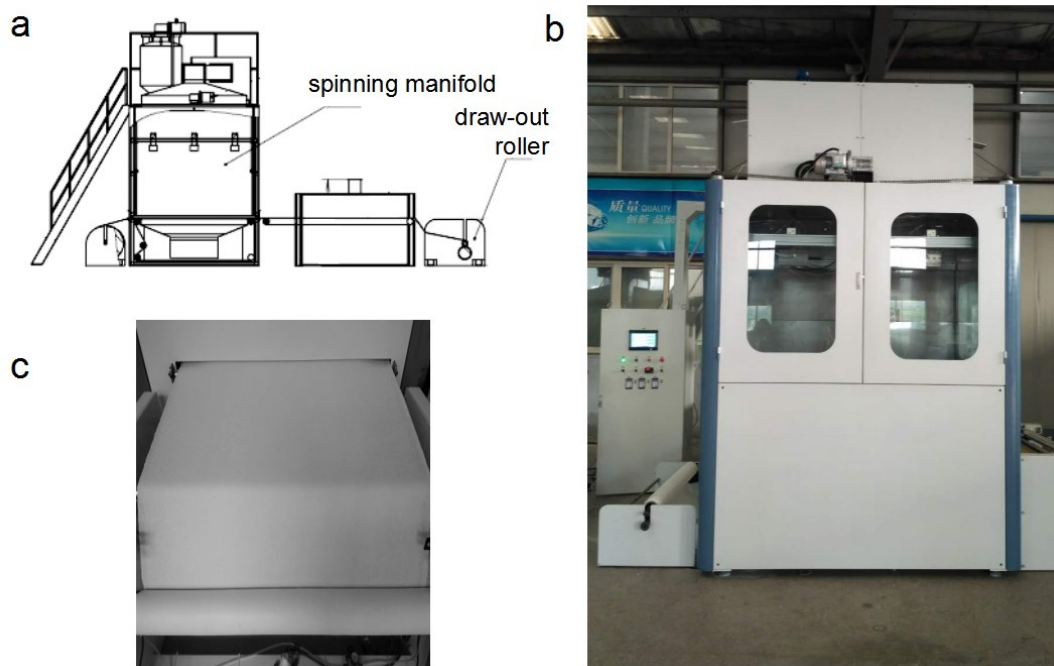


Fig. S1 The layout of the pilot-plant solution blowing equipment (a), a photograph of the spinning manifold (b) and a photograph of the solution-blown PAN nanofiber mat (c).

Gelation of DMDBS.

DMDBS is a well-known low-molecular-weight gelator with butterfly shape, hydrophobic “wings,” and hydrophilic “body.” Its chemical structure is shown in Fig. 1c. DMDBS was dissolved in n-propanol at 80 °C and then cooled to environmental temperature to observe its gel behavior, as shown in Fig. 1c. To observe the morphology, xerogel was obtained by dropping hot solution onto glass sheet for gelation, followed by a further freeze drying. As Fig. S2 shown, DMDBS assembled into nanofibrils and their corresponding nanoweb.

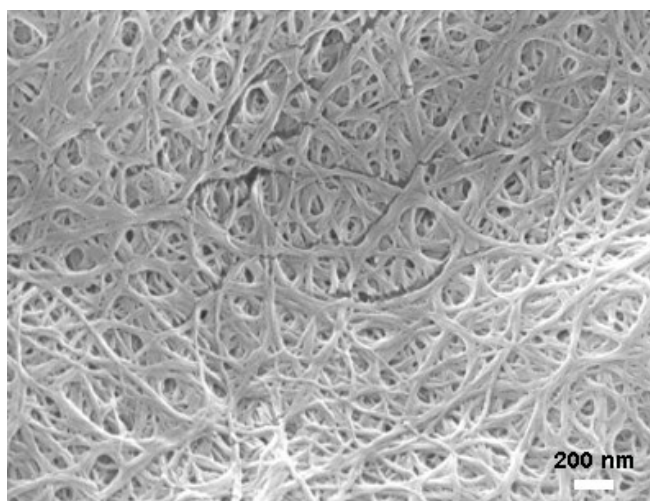


Fig. S2 SEM image of DMDBS xerogel.

Fabrication of the HDNNs

The solution-blown PAN nanofiber mat (PAN-NM) was immersed into DMDBS solutions in n-propanol at 80 °C for saturation with the solution. Then, the PAN-NM containing DMDBS solution was taken out and placed under environmental conditions for gelation. Finally, the residual solvent was removed by vacuum and dried at 60 °C. A similar procedure was used for n-octyl alcohol and ethylene glycol system.

Morphology and structure characterization

The nanofibers and nanofibrils were characterized using Zeiss 1530 FE-SEM equipped with a scanning electron microscope (SEM) detector with an acceleration voltage of 2 kv. The fiber diameters of membranes were determined by utilizing the ipwin32 software.

Pore sizes were measured on a capillary flow porometer for porous materials based on the principle of liquid extrusion porometry. A wetting liquid with a known surface tension of 16 dynes/cm was used. The average values of at least three measurements were obtained. FTIR spectroscopy was measured with the Nicolet 50 FT-IR equipment.

The mechanical property of the filter was measured using a YG004N single-fiber strength meter. Cross-section images were captured using a focused ion beam-SEM dual beam system (FIB-SEM, ZEISS Auriga Compact).

Adsorption model calculation.

Dispersion-corrected density functional theory (DFT-D) calculations were employed to clarify the adsorption behaviour of DMDBS on PAN surface in solvents, which has been verified to get effective evaluation of the noncovalent interactions in liquid systems²⁻⁴. All calculations were performed with the conductor-like screening model (COSMO) approach of DMol³ package implemented in Materials Studio,^{5, 6} where the bulk solvation of n-propanol and ethylene glycol were represented by the values of dielectric constant ϵ that 20.3 and 41.2, respectively. Acrylonitrile tetramer, having large enough interface for the adsorption of DMDBS molecule, was built and chosen as PAN surface. The calculated adsorption models were shown in Fig. S3, and the optimized were shown in Fig. 2b-c.

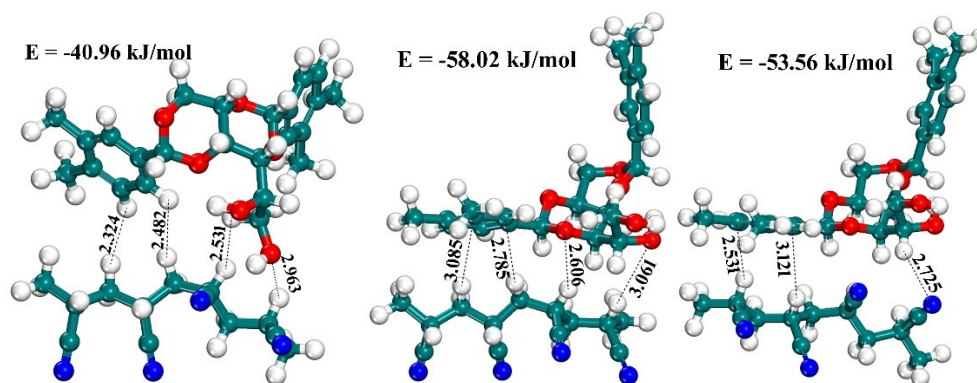


Fig. S3 Calculated adsorption configurations of DMDBS onto PAN surface

Polarizing microscope observation.

A XPN-100E hot-stage polarizing microscope was used to observe the crystallization phenomenon in DMDBS solution. A piece of PAN-NM was placed on a glass slide, some hot DMDBS solution was poured into, and a cover glass was covered. The crystallization phenomenon in the cooling process was observed.

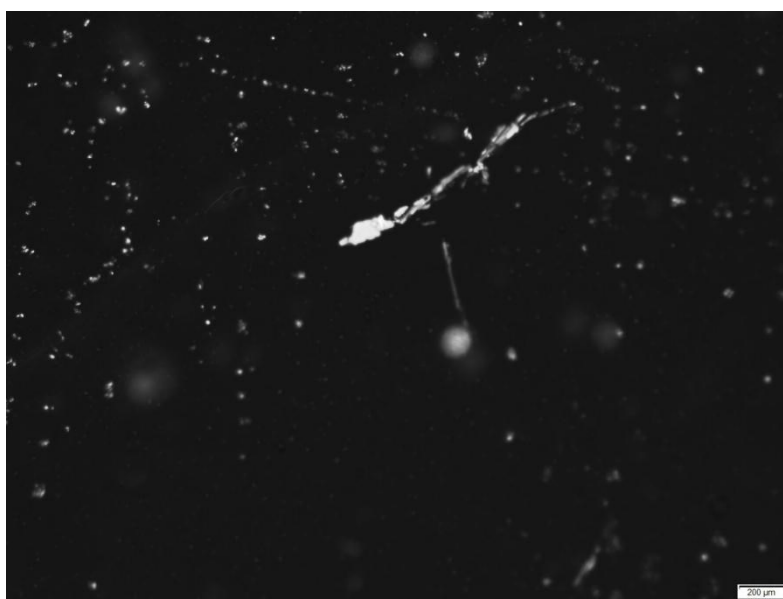


Fig. S4 Polarizing microscope photo of DMDBS solution. In the upper part, PAN nanofibers were involved.

SEM images HDNNs.

To confirm the feasibility of formation of HDNNs in other solvents, 1-octanol ($\epsilon=10.3$) and ethylene glycol ($\epsilon =41.2$) were investigated. As Fig. S5 presented, well-structured HDNNs were obtained with similar procedure.

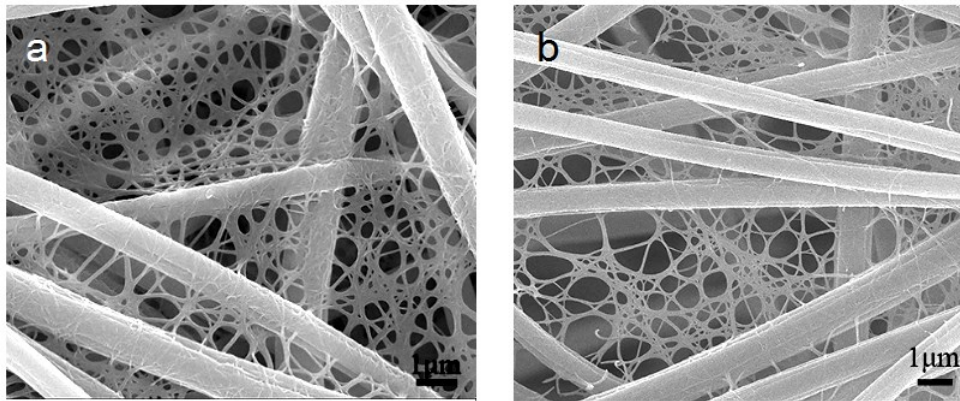


Fig. S5 SEM images of HDNNs using solvents of 1-octanol (a) and ethylene glycol (b).

Young's modulus tested by AFM.

Young's modulus was determined using an AFM microscope (Bruker Dimension Icon) equipped with a silicon probe to identify the mechanical properties of DMDBS nanofibrils. **Fig. S6** exhibits nanoindentation force vs. deformation curves of DMDBS nanofibril. By fitting the curve to Hertzian contact model, Young's modulus of DMDBS nanofibril was obtained with an average value of 58.2 MPa.

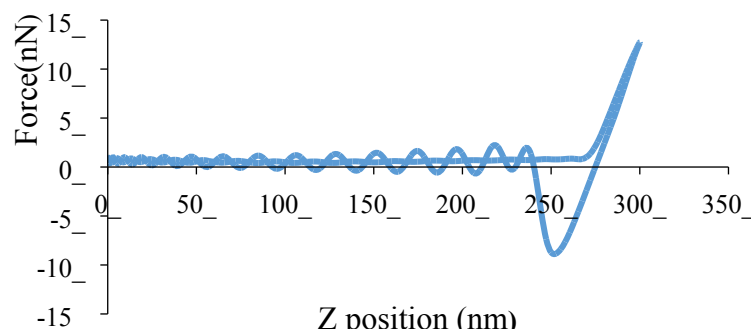


Fig. S6 Force-displacement plot of DMDBS fibrils.

Filtration tests

Filtration efficiency and pressure drop: Filtration performance was first measured using an AFC 131 device (TOPAS, German. Fig. S7). The test sample is a circle with a diameter of 15 cm clamped by two circular plates. The test was performed at 3000 mg/m² particle concentration and with an airflow velocity of 32 L/min. After testing, the overall efficiency and pressure drop were obtained along with the efficiency for different particle sizes.



Fig. S7 The photograph of TOPAS AFC 131 device. (This image is a public photo obtained from the manufacturer's official website)

PM_{2.5} blocking test: To further reveal the PM blocking ability of the HDNNs filters, burning incenses were adopted to simulate highly polluted outdoor environment, and the size of the smoking PMs was measured with an aerosol spectrometer system (Promo 3000 P, PALAS). By collecting the burning PMs in 60s, the size distribution was found from <200 nm to >10 μm , as shown in Fig. S8. In PM_{2.5} blocking test, the PMs concentration was adjusted as about 900 $\mu\text{g}/\text{m}^3$ by blending fresh air with the burning smoke at the gas flowing rate of 600L/min. The inlet and outlet PM counts were detected respectively using two laser PM detectors to calculate the filtration efficiency.

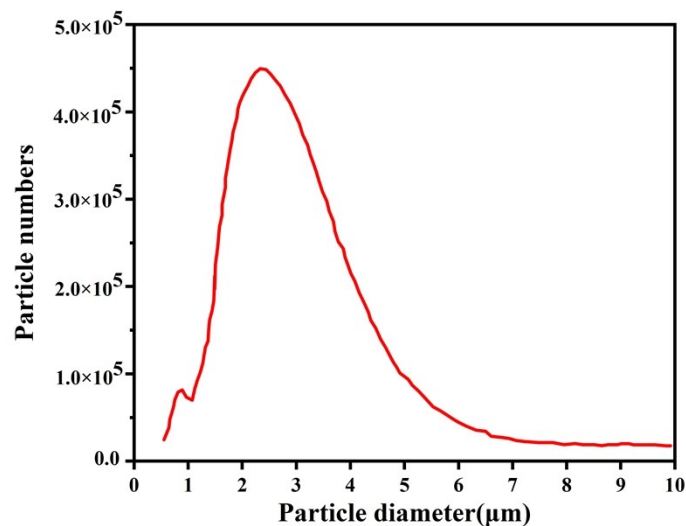


Fig. S8 The size distribution of PMs from the burning incenses

Moisture management tests

Moisture management test (MMT) was further applied using M290 MMT to quantitatively evaluate the water transport performance of the HDNNs. Approximately 9 g of sodium chloride was placed in 1 L of distilled water to prepare the synthetic sweat and to keep the conductivity of the solution at $16 \text{ ms}\pm 0.2 \text{ ms}$. Before the test, the sample was placed on a level surface, and the fabric was conditioned in a standard atmosphere for at least 24 h.

The sample was cut into 8 cm \times 8 cm squares. The humidity-conditioned sample was placed between the top and the bottom sensors. A certain amount of test solution (synthetic sweat) was dropped on the sample, and then, the condition of the solution being transferred was tested in 3D directions on the sample.

Reference

1. Y. C. Duan, J. Song, X. M. Pang, S. J. Sun and R. X. Feng, *Chem. Ind. Eng. (China)*, 2012, **29**, 30.
2. J. Witte, N. Mardirossian, J. B. Neaton and M. Head-Gordon, *J. Chem. Theory Comput.*, 2017, **13**, 2043-2052.
3. B. Van Troeye, M. Torrent and X. Gonze, *Phys. Rev. B*, 2016, **93**, 144304.
4. R. Peverati and K. K. Baldrige, *J. Chem. Theory Comput.*, 2009, **5**, 2772-2786.
5. B. Delley, *J. Chem. Phys.*, 1990, **92**, 508-517.
6. B. Delley, *J. Phys. Chem.* 1996, **100**, 6107-6110.